JOURNAL OF SOLID STATE CHEMISTRY 112, 73–77 (1994)

$YBa_2Fe_3O_8$ with Varied Oxygen Content

P. Karen and A. Kjekshus[1]

Department of Chemistry, University of Oslo, Blindern, N-0315 Oslo 3, Norway

Received June 16, 1993; accepted November 4, 1993

The oxygen content in $YBa_2Fe_3O_{8+w}$ is varied within $-0.2 < w < 0.1$ by thermal equilibration upon controlling the oxygen partial pressure ($10^{-30} < p_{O_2} < 150$ atm) at various temperatures ($950 < T < 1250$ K) and by the getter technique. No decomposition is observed at the upper reached oxygen level. The lower oxygen content limit is estimated as 7.75 per formula unit, evidenced by the first sign of one or more Fe^{2+} phases appearing before the final degradation into metallic Fe. The unit cell volume has a maximum at the stoichiometric oxygen content (corresponding to Fe^{III}), and the (high-temperature) electrical conductivity shows a minimum close to this composition, which is reached below $p_{O_2} = 10^{-12}$ atm for temperatures below 1250 K. In oxygen-rich atmospheres, the conductivity becomes independent of temperature above some 800 K. Magnetic susceptibility measurements confirm the occurrence of antiferromagnetism in $YBa_2Fe_3O_{8+w}$ with $T_N \sim 700$ K, and some irregular features are pointed out.

INTRODUCTION

The crystal structures of $YBa_2Fe_3O_8$ and $YBa_2Cu_3O_7$ are closely related (1). The main difference is that the ferrite structure has a sheet of corner sharing octahedra where cuprate has its square chains, sandwiched between the virtually identical square-pyramidal sheets. Hence, the $YBa_2Fe_3O_8$ structure does not contain (the more common) tetrahedrally coordinated Fe found in $CaLa_2Fe_3O_8$ and related structures (2), and $YBaFeCuO_5$ may be taken as an example of another phase with the square-pyramidally coordinated iron (3). Oxygen-saturated $YBa_2Fe_3O_{8+w}$ has a minor excess of some 0.07 oxygens per formula unit (4) and these extra-oxygen atoms have been located by powder neutron diffraction (5, 6) as interstitial defects in the Y-layer. This is an important feature which possibly may have major effects on, e.g., transport properties of $YBa_2Fe_3O_8$. The extent of the oxygen nonstoichiometry as a function of temperature and partial pressure of oxygen is therefore of obvious interest, as well as the related unit cell data and other physicochemical properties. High-temperature electrical conductivity and magnetic susceptibility measurements complement the compositional and structural information provided in this study.

[1] To whom correspondence should be addressed at Department of Chemistry, University of Oslo, Blindern, P.O. Box 1033 N-0315 Oslo, Norway.

EXPERIMENTAL

Samples were prepared by firing of precursor materials obtained from liquid mixed citrates. Y_2O_3 (5N, Megon) and $BaCO_3$ (reagent grade, Merck) were dissolved in boiling citric acid monohydrate (reagent grade, Fluka), and a concentrated solution of iron citrate was added, prepared from Fe metal (99.9+%, Aldrich Chemicals) as reported previously (4). The clear citrate melt was dehydrated at 180°C, the product was milled and incinerated in air at 450°C. The precursor was pressed into pellets and fired at 970°C three times for 100 hr, in flowing CO_2-free oxygen (4).

The oxygen content was controlled by two different means: (i) by varying the temperature and oxygen partial pressure upon dilution–mixing or compressing of the gas atmosphere ($10^{-30} < p_{O_2} < 150$ atm) and (ii) by a getter technique. (i) For atmospheric and lower pressures, a gas-mixing station was used to dilute Ar(<2 ppm O_2) with either hydrogen (99.995%) or oxygen (99.9%), in up to three mixing steps. The gas mixture was wetted to $p_{H_2O} = 0.02$ atm by passing it through 42.5 wt% H_3PO_4. The small variations in the p_{H_2O}, occurring owing to changes in the temperature and concentration of the phosphoric acid were included in calculations of p_{O_2} with the program GASMIX (7). The equilibration time for the small (7-mm-diameter) porous (some 50%) pellets was minimum 24 hr at 674, 900, and 977°C, followed by rapid cooling in the same atmosphere. The cooling half-time (in °C) was some 5 minutes and, according to electrical conductivity measurements, this is well below the rate of the diffusive processes in the sample. Increased oxygen pressures were applied at 450°C (1 week equlibration). A p_{O_2} of ~10 atm was obtained in a silica ampoule with $Ag_2O + \frac{1}{10}BaO_2$, and $p_{O_2} \approx 150$ atm was created in a silica-lined steel autoclave by connecting it directly with the oxygen (pressure) cylinder. The oxygen annealed samples were quenched at rates of some 200°C per sec for atmospheric and lower

0022-4596/94 $6.00

pressure, and some 20°C per sec for the elevated pressures. (ii) The getter technique used calculated amount of Ti or Misch Metal contained together with the sample in closed silica ampoules (Ti: Koch-Light, 100–150 μm fraction, at 800–950°C; Misch Metal: Treibacher Chemische Werke, Austria, at 400–500°C). The equilibration time was 1 week.

The oxygen content of all samples was analyzed cerimetrically, either by a direct titration of the as present Fe^{II} content with ferroin as an indicator or by a titration of the remaining excess of Fe^{II} from added Mohr's salt when Fe^{IV} was present in the sample. The dissolution of the samples in 3 *M* HCl was carried out in an Ar atmosphere at 50°C, promoted by ultrasound stirring. The overall iron content in the samples was determined in parallel, after a quantitative reduction of all present Fe into Fe^{II} by $SnCl_2$.

The phase purity and unit cell parameters of each sample were evaluated from powder X-ray diffraction (PXD), using a Guinier–Hägg camera with Cu$K\alpha_1$ radiation and Si as an internal standard.

Electrical conductivity was measured by the four-point van der Pauw method (8), at temperatures up to 1000°C upon varied oxygen partial pressures. The sample was cold pressed by a load of 8 tons and sintered 4 days in oxygen at 1020°C. The 21.6 mm in diameter, 2.35 mm thick disc was provided with four gold point-contacts, which were pressed equidistantly around the brim by a corundum plate with corundum stirrups on steel springs at the cold end. The ac conductivity (123 Hz, 1 V amplitude) was measured with a HP-4192 impedance bridge and was corrected for the sample porosity p by dividing with the square of the ratio of apparent and X-ray densities [corresponding to $(1 - p)^2$; $p = 0.41$ as determined].

Magnetic susceptibility was measured in the temperature interval $80 < T < 1000$ K with a Faraday balance (maximum field 8 kOe, 15–30 mg samples). The powder samples were vacuum sealed in silica-glass ampoules during the measurements.

RESULTS AND DISCUSSION

$YBa_2Fe_3O_{8+w}$ synthesized at ambient oxygen pressure has an oxygen content of around $w = 0.08$ per formula which could be increased only slightly (up to $w = 0.11$) by the treatment at elevated oxygen pressures (Fig. 1). On the other hand, the oxygen content can be decreased more profoundly by a decrease in p_{O_2}. The variation of the room-temperature unit cell parameters with the oxygen content parameter w of $YBa_2Fe_3O_{8+w}$ is illustrated in Fig. 1. A maximum in the unit cell volume occurs at the exact stoichiometric composition $YBa_2Fe_3O_8$, with a more rapid decrease in the oxidized region than in the reduced region. The compositional changes in the cell

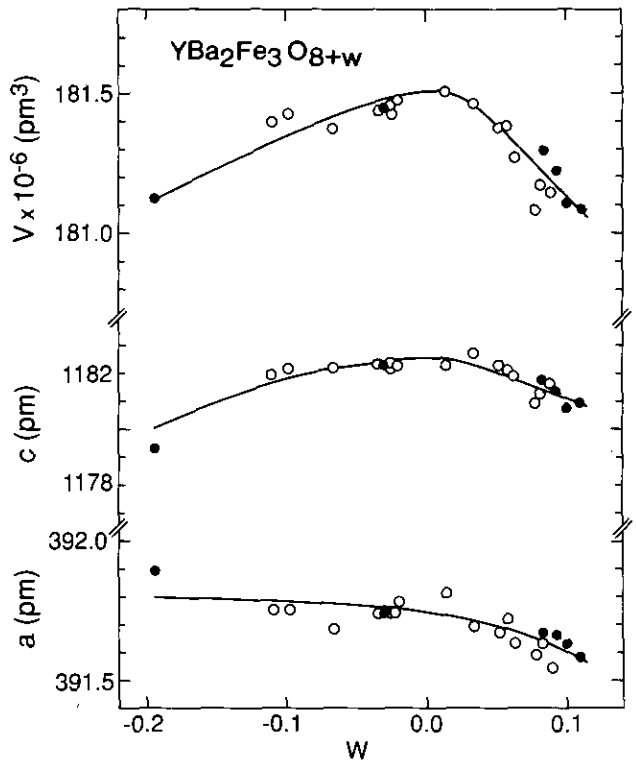

FIG. 1. Unit cell parameters of $YBa_2Fe_3O_{8+w}$ as functions of w. (Open circles—samples equilibrated at various temperatures under fixed oxygen partial pressures by gas-mixing; see also Table 1. Closed circles—large scale samples made using: Ti-gettering, Misch Metal-gettering, 1 atm O_2, 1 atm O_2, 10 atm O_2, 150 atm O_2, in order of increasing oxygen content.)

parameters are rather subtle, and, as a result Fig. 1 gives an unjust impression of the actually fairly precise data.

The oxidized powder samples assume a dark, brown–violet color, which lightens upon reduction to oxygen contents around eight per formula, whereupon the color turns black on further reduction. The oxidized samples do not sinter easily, even close to the decomposition temperature of ~1100°C (4), and the powders exhibit an unusually low internal friction, consistent with the layered character of the structure. A decrease in the solidus temperature occurs for the most reduced samples, manifested in sintering at temperatures well below 1100°C. This sintering is not accompanied by any significant discontinuous change in the unit cell parameters, as may be judged from Table 1. However, the powders of the sintered products do not retain the low internal fraction characteristic of the samples synthesized in oxygen, and certain minor structural changes of an order/disorder nature probably take place.

An estimate of the lower composition limit for the $YBa_2Fe_3O_{8+w}$ phase with respect to w was attempted using both the gas-mixing and getter techniques for oxygen content control. The lowest oxygen content in Table 1 (for the

TABLE 1
Oxygen Content and Unit Cell Parameters of $YBa_2Fe_3O_{8+w}$ as Functions of Temperature and Partial Pressure of Oxygen

t (°C)	log p_{O_2}	log p_{Ar}	log p_{H_2}	$8 + w$	a (pm)	c (pm)	Note
977	−0.0088	Ar absent	−9.159	8.09(1)	391.54(4)	1181.6(2)	Brown–violet
900			−9.844	8.08(1)	391.59(4)	1180.9(2)	Brown–violet
674			−12.5	8.08(1)	391.63(4)	1181.2(2)	Brown–violet
900	−5.69		−7.005	8.06(1)	391.63(3)	1181.9(2)	Red–brown
674	−5.70		−9.655	8.06(1)	391.72(2)	1182.1(1)	Red–brown
977	−9.02	−0.0088	−4.653	8.05(1)	391.67(5)	1182.3(2)	Light brown
674	−15.70			8.03(1)	391.69(3)	1182.7(1)	Light brown
977	−11.71	−0.0090	−3.308	7.934(5)	391.68(5)	1182.2(2)	Dark, compact
900	−13.08			7.966(5)	391.74(3)	1182.3(1)	Light brown
674	−18.39			8.01(1)	391.81(5)	1182.3(2)	Light brown
900	−14.67	−0.0102	−2.515	7.975(5)	391.74(3)	1182.4(1)	Light brown
674	−19.98			7.976(5)	391.74(3)	1182.2(1)	Light brown
900	−16.80	−0.0249	−1.447	7.816(5)	392.19(13)	1178.9(7)	Dark, compact
674	−22.12			7.980(5)	391.78(2)	1182.3(1)	Light brown
900	−18.59	−0.1550	−0.553	6.493(5)	—	—	$Fe^{+2.00}$, green
674	−23.90			7.902(5)	391.75(2)	1182.1(1)	Darker brown
674	−24.99	Ar absent	−0.0088	—	—	—	Fe metal

Note. To the pressure values (in atm) listed, $p_{H_2O} = 0.020$ should be added for all series. Standard deviations appear in brackets; for chemical analyses as estimated from the reproducibility of the titration, for unit cell parameters as calculated.

phase-pure sample) corresponds to $w \approx -0.2$, and, since the dependence of the oxygen content on p_{O_2} is quite steep at the reduced end, *vide infra*, more profound deoxidations were attempted by a fine-scaled gettering at 900°C. Samples intended to acquire oxygen contents of 7.65 and 7.60 were partially decomposed upon formation of a green admixture. Assuming Fe^{II} in the admixture, the lower limit for the oxygen content at 900°C may be estimated as close to 7.75 per formula ($w = -0.25$). Upon careful variations in the partial pressure of oxygen at 900°C, the green-colored product can be obtained in the "pure" state, containing exactly Fe^{2+} according to the chemical analysis. Further reduction leads to metallic Fe accompanied (at 675°C) by a perovskite-type phase with $a = 420$ pm. Attempts to index the PXD diagram of the green product as a single phase were unsuccessful even when monoclinic symmetry was tried. The perovskite-type phase is apparently related to the nonexistent $BaYO_3$, as implied by the size of the unit cell, and it is probably stabilized by an OH^- incorporation originating from the wetted hydrogen.

Oxygen-saturated $YBa_2Fe_3O_{8.08}$ is a semiconductor at room temperature ($\sigma = 4 \times 10^{-2}$ S/cm at 284 K). Above 800–820 K, σ becomes virtually temperature independent (Fig. 2), and this behavior is maintained even when the oxygen content is slightly reduced, but still above 8 per formula unit. From Fig. 3 and its inset, it is seen that the log σ vs log p_{O_2} isotherms go through minima at or near the exact stoichiometry $YBa_2Fe_3O_{8.00}$. Below this oxygen content, the dependences suggest n-type semiconductivity, whereas the linear increase in log σ with log p_{O_2}, expected for p-type, is noted only very slightly above the $YBa_2Fe_3O_{8.00}$ stoichiometry. Instead, a saturation plateau is observed, similar to that formed by a presence of acceptor defects. This is a very common situation for assumed "pure", "undoped" oxides and an impurity (say Ca or Sr from $BaCO_3$) and/or a Y/Ba mismatch may be the source of the defects. Judging from, e.g., the conductivity of $SrFeO_3$ [$\sim 10^3$ S/cm (9)], the concentration of the acceptor defects need not to be higher than some 0.5

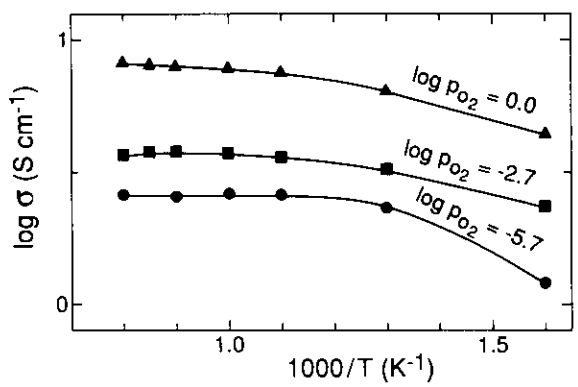

FIG. 2. Temperature dependence of the electrical conductivity of $YBa_2Fe_3O_{8+w}$ at log $p_{O_2} = 0.0$, −2.7, and −5.7 atm (denoted by ▲, ■, and ●, respectively).

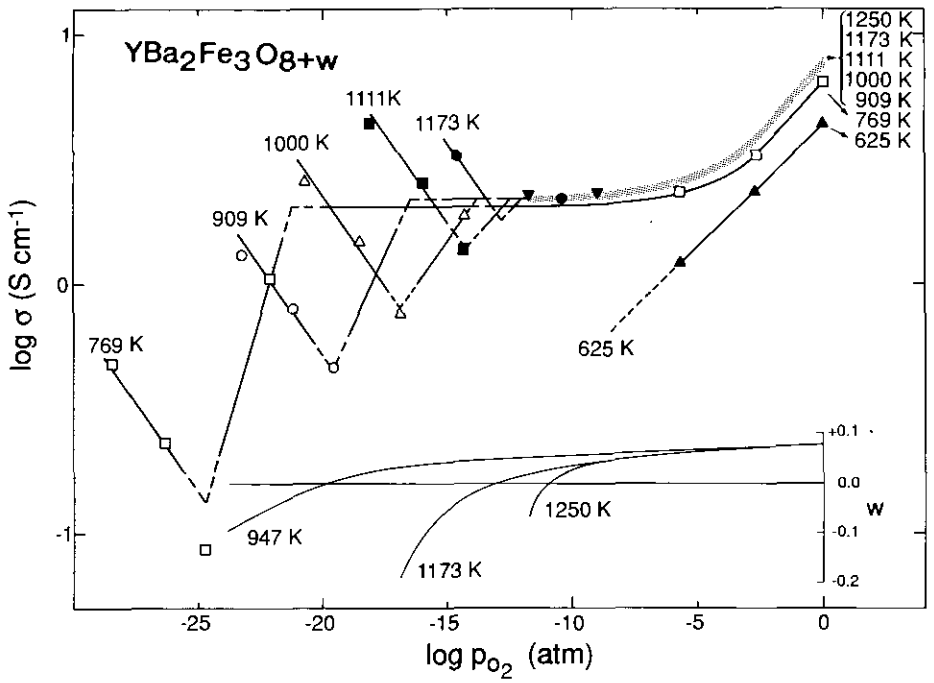

FIG. 3. Electrical conductivity of $YBa_2Fe_3O_{8+w}$ at various temperatures and partial pressures of oxygen. [For clarity, experimental points and conductivity isotherms are not shown in the shaded region, but the order of curves follows the temperature sequence. The inset of log p_{O_2} vs w (see Table 1) is shown for comparison.]

mole% to explain the saturation value of 5 S/cm for $YBa_2Fe_3O_{8+w}$.

All, as-synthesized (viz., subject to free cooling inside the furnace), samples exhibit antiferromagnetism with a Néel temperature (T_N) around 700 K. The temperature dependence of inverse magnetic susceptibility is illustrated on one of the pressure-oxidized samples ($YBa_2Fe_3O_{8.11}$) in Fig. 4, and shows a notable feature: On heating, $\chi^{-1}(T)$ follows branch 1 in Fig. 4, but after the Néel temperature is reached and the paramagnetic regime (branch 2) entered, the sample follows branch 3 instead of branch 1 upon cooling below T_N. From then on, the sample behaves reproducibly upon repeating the cycle within the temperature range of the original measurement, following branches 3 and 2 on heating and branches 2 and 3 on cooling. In a series of experiments, we established that: (i) an as-synthesized sample must be heated above T_N in order to acquire the $\chi^{-1}(T)$ dependence characteristic of branch 3; (ii) no heat treatment below T_N can revert the acquired branch 3 behavior back to the original branch 1; (iii) analogous changes in magnetic behavior are found for samples with various oxygen contents; and (iv) the effects concerned are not rooted in structural distinctions which can be identified by PXD. Hence, the as-synthe-

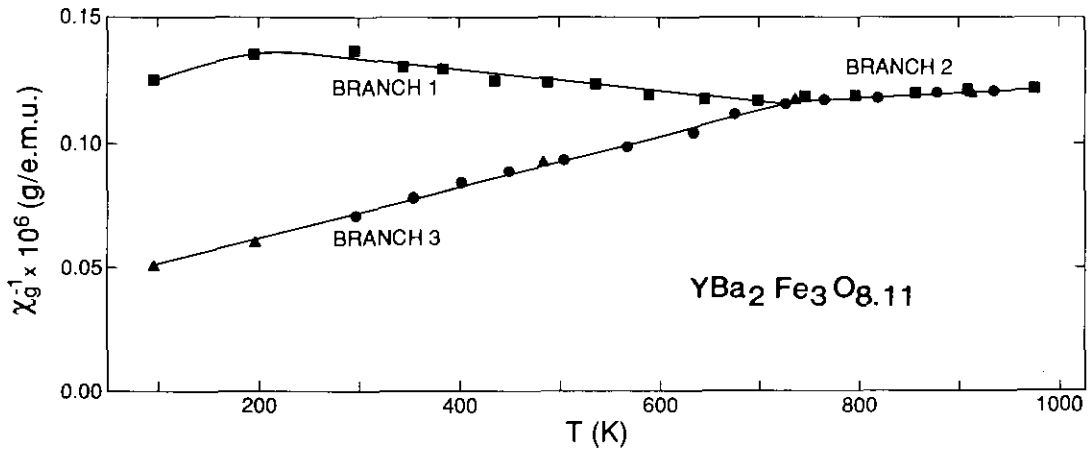

FIG. 4. Temperature dependence of inverse magnetic susceptibility for oxygen saturated $YBa_2Fe_3O_{8.11}$; for the different branches, see text.

sized $YBa_2Fe_3O_{8+w}$ must be subject to a kind of "quenched" high-temperature disorder in the oxygen substructure. In the search for the "order–disorder" temperature, a series of magnetic susceptibility measurements has been performed on samples heated in oxygen, at first for a prolonged time at 1273 K (to ascertain the assumed disordered state), then annealed for 2 days at selected lower temperatures and quenched. The temperature was lowered for each subsequent annealing of the originally identical sample. The results show rather continuous changes between the two types of behavior (1, 2 vs 3, 2, Fig. 4), and suggest that in the region between some 800–1000 K there is an OD change which concerns some of the used and potentially available oxygen sites in the $YBa_2Fe_3O_{8+w}$ structure. Another sign of similar phenomena is manifested in a degree of irreproducibility of structural and magnetic properties of $Y_{0.9}Ca_{0.1}Ba_2O_{8.05}$ when heated above 675 K (5). It is also conceivable that the remanent magnetization and the difference between field and zero-field cooling for a nominally $YBa_2Fe_3O_8$ sample (10) may have a similar origin. [On the other hand, no significance is attached to magnetic properties reported in Ref. (11) since this contribution gives wrong oxygen content ($7 + w$), lattice symmetry (orthorhombic), and Néel temperature (1020 ± 10 K) for the YBFO phase.]

In conclusion, it may be stated that the established existence of the oxygen-content homogeneity region provides the $YBa_2Fe_3O_{8+w}$ phase with an interesting variation of properties. Comparisons with the charge doping of the superconducting cuprates are of obvious interest, and work is in progress to study the crystal and magnetic structures of the reduced variants by powder neutron diffraction (6).

REFERENCES

1. Q. Huang, P. Karen, V. L. Karen, A. Kjekshus, J. W. Lynn, A. D. Mighell, N. Rosov, and A. Santoro, *Phys. Rev. B: Condens. Matter* **45,** 9611 (1992).
2. J. C. Grenier, F. Menil, M. Pouchard, and P. Hagenmüller, *Mater. Res. Bull.* **12,** 79 (1977).
3. L. Er-Rakho, C. Michel, P. Lacorre, and B. Raveau, *J. Solid State Chem.* **73,** 531 (1988).
4. P. Karen, P. H. Andresen, and A. Kjekshus, *J. Solid State Chem.* **101,** 48 (1992).
5. I. N. Sora, Q. Huang, J. W. Lynn, N. Rosov, P. Karen, A. Kjekshus, V. L. Karen, A. D. Mighell, and A. Santoro, *Phys. Rev. B: Condens. Matter,* **49,** 3465 (1994).
6. Q. Huang, P. Karen, V. L. Karen, A. Kjekshus, J. W. Lynn, A. D. Mighell, I. N. Sora, N. Rosov, and A. Santoro, to be published.
7. T. Norby, "The IS/ISPLOT/GASMIX Package of Programs," Center for Materials Research, University of Oslo, Norway, 1992.
8. L. J. van der Pauw, *Phillips Tech. Rev.* **20,** 220 (1958/1959).
9. J. B. Goodenough, *Czech. J. Phys. Ser. B.* **17,** 304 (1967).
10. I. Felner, I. Nowik, U. Yaron, O. Cohen, E. R. Bauminger, T. Kroener, and G. Czjzek, preprint.
11. M. ElMassalami, A. Elzubair, H. M. Ibrahim, and M. A. Rizgalla, *Physica C (Amsterdam)* **183,** 143 (1991).